

REPORT

QUANTUM OPTICS

Coherent single-atom superradiance

Junki Kim, Daeho Yang, Seung-hoon Oh, Kyungwon An*

Superradiance is a quantum phenomenon emerging in macroscopic systems whereby correlated single atoms cooperatively emit photons. Demonstration of controlled collective atom-field interactions has resulted from the ability to directly imprint correlations with an atomic ensemble. Here we report cavity-mediated coherent single-atom superradiance: Single atoms with predefined correlation traverse a high-quality factor cavity one by one, emitting photons cooperatively with the N atoms that have already gone through the cavity (N represents the number of atoms). Enhanced collective photoemission of N -squared dependence was observed even when the intracavity atom number was less than unity. The correlation among single atoms was achieved by nanometer-precision position control and phase-aligned state manipulation of atoms by using a nanohole-array aperture. Our results demonstrate a platform for phase-controlled atom-field interactions.

Superradiance is a collective radiation phenomenon by a number of quantum emitters (I). In the original prediction, exchange symmetry is present in closely packed emitters whose interparticle distance is much smaller than the transition wavelength, and therefore dipole-dipole correlation emerges during their spontaneous decay process. The correlation makes the ensemble behave collectively and induces enhanced interaction with the vacuum fields, leading to stronger and faster radiation emission compared with the ordinary spontaneous emission. Early experiments performed with a large number of emitters (as in a dense atomic vapor or in a beam) reported observations consistent with the prediction ($2, 3$). Recent technical advances have enabled the realization of superradiance in various systems, such as a Bose-Einstein condensate (4), quantum dots (5), and trapped atoms coupled to a cavity (6).

The mutual phase correlation among atoms is the key to superradiance: It can make the ensemble behave as a single macrodipole. Moreover, direct control of atomic phases enables controllable collective atom-field interactions. In recent experiments, the phase of atoms in an ensemble was imprinted by a single-photon pulse ($7-9$) or a frequency-swept laser pulse (10). The ensemble then started superradiant emission without a threshold or an initial time delay. The output field in this case follows the given imprinted phase, and thus its spatial mode overlaps with the input mode, making it hard to spatially distinguish the input and output fields. This approach works only in the pulsed regime. Observation of a superradiant state in a Bose-Einstein condensate coupled to a cavity was another notable discovery (11). However, this work relied on self-organization of atoms

on the basis of a thermodynamic principle, and thus further tunability could not be attained.

Another approach to achieve controllable superradiance is preparation of emitters in a cavity and manipulation of the quantum state of individual emitters. Ions (12), neutral atoms (13), and artificial atoms based on superconducting circuits (14) have been used in this approach. The results include immediate strong and fast radiation emission and controllability between superradiance and subradiance. However, technical difficulties have limited the number of emitters involved in the superradiance to only two.

We present an approach to realize phase-controlled superradiance whereby single atoms are prepared in the same quantum superposition of ground and excited states and traverse a cavity one by one. The long-lived cavity field then mediates collective interaction among the phase-correlated single atoms separated in time, leading to superradiance. The collective interaction is one-sided in that the emission of a particular atom in the cavity is cooperative only with the preceding atoms. Even when, at most, only one atom is present in the cavity, tens of atoms participate in the superradiance, and the emission intensity is proportional to the square of the number of the participating atoms.

Our system, adapted from (15), consists of a supersonic barium atomic beam and a high-quality factor optical cavity with which the atoms resonantly interact (Fig. 1A). The ^{138}Ba atoms are prepared in a superposition state of the ground and excited states just before they enter the cavity mode by a pump laser propagating perpendicular to the cavity axis as well as to the atomic beam direction. The atomic phase imprinted by the pump laser depends on the position at which the atom traverses the pump laser. The phase of the atom-cavity coupling also alternates 0 and π rad, following the standing wave structure of the cavity mode. A checkerboard-pattern nanohole array is used as an atomic

beam aperture to localize and control the atomic position. The localized atoms then selectively pick up the phase of the pump laser as well as the cavity field corresponding to their positions prescribed by the array structure. As a result, the atom-field relative phase is the same for every atom traversing the cavity (Fig. 1B). The desired atomic internal state is prepared by the pump laser with a pulse area of $\Theta = \int |\Omega_p(x)/v| dx$, where $\Omega_p(x)$ is the Rabi frequency due to the pump laser and v is the velocity of the atom. The atomic state can then be expressed as $|\psi_{\text{atom}}\rangle = \sin(\Theta/2)|e\rangle + \cos(\Theta/2)\exp(i\phi)|g\rangle$, where ϕ is the atomic phase imprinted by the pump laser. Atomic correlation between any two of the injected atoms is then given by $\langle\sigma_i^\dagger\sigma_j\rangle = 1/4\sin^2\Theta$ (where $\sigma_i = |g\rangle\langle e|$ is the lowering operator of the i th atom, σ_j corresponds to the j th atom, and \dagger indicates the Hermitian conjugate), showing that the atom-atom correlation is maximized when $\Theta = \pi/2$.

Injected atoms then emit photons into the cavity mode and build up the cavity field. A previous study assuming a lossless cavity expected enhanced collective emission by consecutively injected N atomic dipoles to show explicit N^2 dependence (N , number of atoms) (16). The long-lasting cavity field links the atoms together, and the expected photon number is exactly the same as that of simultaneously injected N dipoles (fig. S1).

When a cavity has a finite decay, the gain (emission by atoms) and the loss (absorption by atoms, as well as the cavity decay) of the cavity field would be balanced in its steady state. The averaged cavity photon number $\langle n \rangle$ in the steady state can be obtained from the quantum master equation (17) and is approximately given by

$$\langle n \rangle \approx \frac{\langle N_c \rangle \rho_{ee} (g\tau)^2}{2 - (2\rho_{ee} - 1)\langle N_c \rangle (g\tau)^2} + (\langle N_c \rangle |\rho_{eg}| g\tau)^2 \quad (1)$$

where $\langle N_c \rangle \equiv r/\gamma_c$ is the mean number of atoms injected into the cavity during the cavity-field decay time $1/\gamma_c$, with r the atomic injection rate; ρ_{ee} and ρ_{eg} are the density matrix elements of atomic state, with the subscripts e and g representing excited and ground states, respectively; g is the atom-cavity coupling constant; and τ is the atom-cavity interaction time.

The first term, approximately proportional to $1/2\langle N_c \rangle$ when $\langle N_c \rangle (g\tau)^2 \ll 1$, is due to the noncollective emission of atoms, including spontaneous and stimulated emission as well as the cavity quantum electrodynamics effect. The second term, exhibiting a quadratic dependence on $\langle N_c \rangle$, is due to collective emission—that is, the superradiance. Compared to the case with a lossless cavity (16), the number of atoms participating in the superradiance is identified to be $\langle N_c \rangle$ in our study (17). When $\langle N_c \rangle \gg 1$, the second term dominates the emission, and the field state approximately becomes a coherent state $|\alpha\rangle$ with $\alpha = -i\langle N_c \rangle \rho_{eg} g\tau$.

The mean intracavity atom number $\langle N \rangle$ is related to $\langle N_c \rangle$ as $\langle N \rangle = \langle N_c \rangle / (\gamma_c \tau)$. If the cavity-field decay time $1/\gamma_c$ is much larger than τ ($\gamma_c \tau \ll 1$), $\langle N_c \rangle$ can be much greater than unity, even when

Department of Physics and Astronomy and Institute of Applied Physics, Seoul National University, Seoul 08826, Republic of Korea.

*Corresponding author. Email: kwan@phya.snu.ac.kr

the mean intracavity atom number $\langle N \rangle$ is less than unity, and thus the collective effect can take place. The cavity field mediates the collective behavior among the time-separated $\langle N_c \rangle$ atoms that are going through the cavity individually during the cavity-field decay time, leading to the single-atom superradiance. On average, 22 atoms are involved in the collective emission when a single atom is present in the cavity mode.

In our experiment, the phase-aligned atomic dipoles prepared with the aforementioned nanohole array were injected into the cavity, and the mean intracavity photon number in the steady state was measured with a single-photon-counting module. The atom-cavity interaction was in the strong coupling regime with $(g, \gamma, \gamma_c) = 2\pi \times (290, 25, 75)$ kHz, where g is the atom-cavity coupling averaged over the atomic distribution centered around the antinodes of the cavity and γ (γ_c) is the atomic polarization (cavity-field) decay rate. The single-atom cooperativity was $C = g^2/\gamma\gamma_c = 44$. The mean travel time of atoms from the pump to the cavity field was ~ 200 ns, whereas the mean atom-cavity interaction time $\tau = 101$ ns. As a comparative counterpart, we also performed the experiment with a rectangular atomic beam aperture (dimensions: $250 \mu\text{m}$ by $25 \mu\text{m}$) for the case of atoms with random phases. In the latter scenario, the atomic beam was injected into the cavity mode with a small tilt angle to induce Doppler shifts so as to achieve a uniform atom-field coupling (18–21), whose strength is half of the maximum coupling strength.

The collective emission described by the second term in Eq. 1 is expected to have the quadratic dependence on two parameters: the induced atomic dipole moment $\propto |\rho_{eg}|$ and the atom number $\langle N_c \rangle$. First, we investigated $|\rho_{eg}|$ dependence of collective emission by varying the pump pulse area (Fig. 2). Owing to the relation $|\rho_{eg}| = |\frac{1}{2}\sin\Theta|$ for the prepared superposition state, the atomic dipole moment would be maximized with equal ground- and excited-state populations ($\Theta = 0.5\pi$ or 1.5π) and so would be the collective emission. Clear enhancement was observed when the atoms were prepared in the phase-aligned superposition states. The enhancement was more than a factor of 10 for $\Theta < 0.3\pi$ (fig. S2). Combined contributions by ρ_{ee} (noncollective) and $|\rho_{eg}|$ (collective) make $\langle n \rangle$ maximized near $\Theta \approx 0.7\pi$. Owing to the small overlap between the pump laser field and the cavity mode (both are Gaussian), the collective emission process is somewhat disturbed by the stray pump field in the cavity when the pump intensity is strong, which results in the enhancement reduction for $\Theta > \pi$. On the other hand, in the random-phase scenario, the photon number is given by the noncollective emission only, and thus it is maximized with fully inverted atomic states ($\Theta = \pi$).

The enhancement is strongly dependent on the atomic phase purity. In reality, there are several sources of phase noise. Finite atomic localization sets the lower bound of atomic phase variance. Atomic spontaneous emission into free space also contributes to phase diffusion of atoms,

reducing $|\rho_{eg}|$ by 6%. In addition, the pump laser has a phase uncertainty: the laser phase diffuses in time with a finite laser linewidth. If we intentionally make the pump laser linewidth larger, the superradiant enhancement becomes smaller (fig. S3). We performed quantum-trajectory simulation as well as quantum master equation calculation with the experimental parameters, and our data correspond to the numerical results (17) (fig. S4).

Figure 3 shows the mean intracavity photon number $\langle n \rangle$ versus the excited-state atom number $\langle N \rangle \rho_{ee}$. When the atoms have no dipole moment (Fig. 3B), only the noncollective emission is present. With a small number of atoms, the cavity field is primarily made by spontaneous emission of atoms (dashed line), and its photon number increases linearly with the atom number. As the accumulated photon number gets larger, stimu-

lated emission and absorption become dominant over the spontaneous emission, and the system lases for positive inversion ($\rho_{ee} - \rho_{gg} > 0$) or the photon number plateaus for negative inversion ($\rho_{ee} - \rho_{gg} < 0$). Especially for positive inversion, a rapid growth of the photon number starts to occur at $\langle n \rangle \approx 1$, which is the well-known lasing threshold in conventional lasers (22).

However, when atoms have the same phase (Fig. 3A), photon emission is enhanced nonlinearly, with its log-log slope becoming steeper than unity. The measured intracavity photon numbers are consistently larger than the photon number made only by the cavity-enhanced spontaneous emission (dashed line). When the pump pulse area is 0.5π , corresponding to $|\psi_{\text{atom}}\rangle \approx [|e\rangle + \exp(i\theta)|g\rangle]/\sqrt{2}$, the observed log-log slope is 1.66 ± 0.01 . After subtracting the contribution by the noncollective emission

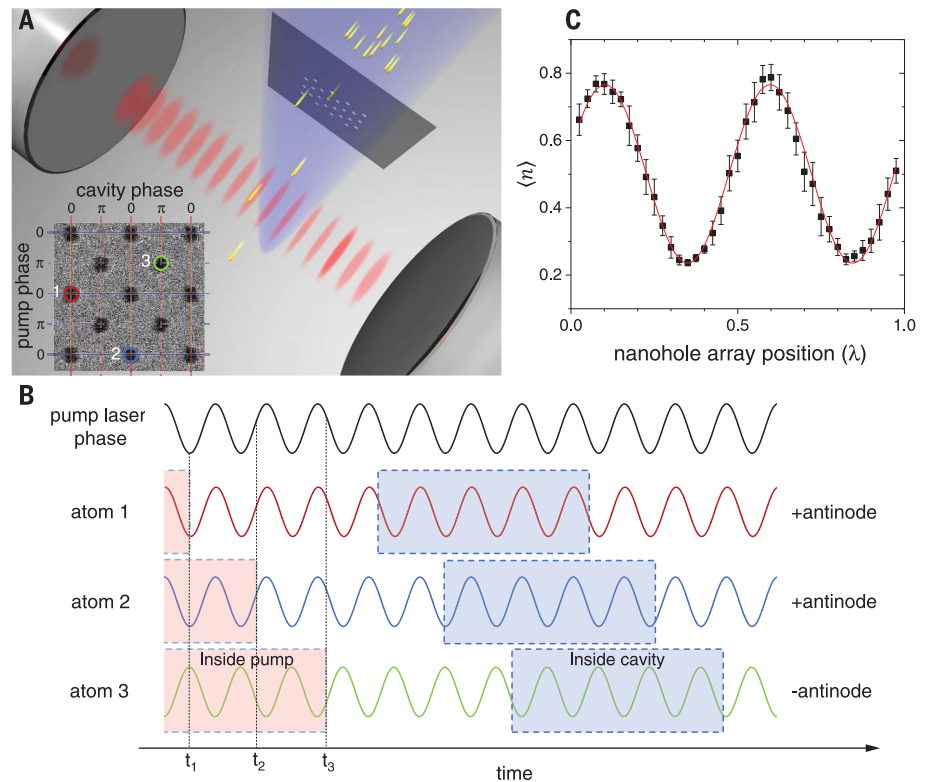


Fig. 1. Phase-controlled atom-cavity interaction with a nanohole-array aperture. (A) Barium atoms (yellow “flying” spheres) go through a nanohole-array aperture and are prepared in a desired state by a pump laser (blue beam). The atoms interact with the cavity field in a given interaction time τ and emit photons into the cavity mode in both collective and noncollective ways. The inset shows a focused ion beam image of the nanohole-array aperture (17). The nanohole-array dimension is 25λ by 25λ , spanning $19.8 \mu\text{m}$ both horizontally and vertically. Here, $\lambda = 791 \text{ nm}$ is the atomic transition wavelength. (B) The atom-cavity relative phase is prescribed by the array structure. Consider three atoms going through nanoholes 1, 2, and 3, as indicated in (A), and then exiting the pump field at times t_1 , t_2 , and t_3 , respectively. The pump laser phase at one of the zero-phase planes is shown with the imprinted atomic phases. Although atom 3 has the opposite imprinted phase compared with the others, it goes through an antinode that is opposite in phase to the antinodes through which atoms 1 and 2 travel. As a result, all three atoms would have identical atom-cavity relative phases. (C) Varying the nanohole-array position along the cavity axis changes the atomic trajectory from crossing nodes to crossing antinodes, and therefore the cavity mean photon number (black square) varies sinusoidally when pumped by fully excited atoms. The signal visibility is 0.54, and the corresponding effective atomic distribution has a full width at half maximum of 0.29λ . The red solid line is a sinusoidal fit to the data. Error bars indicate SD.

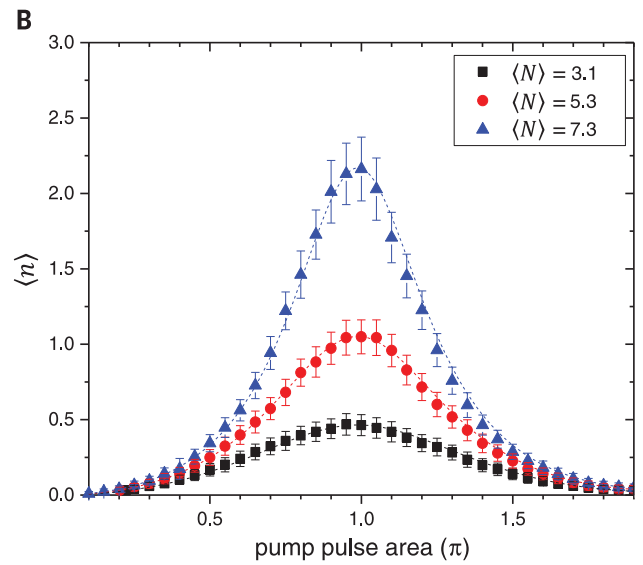
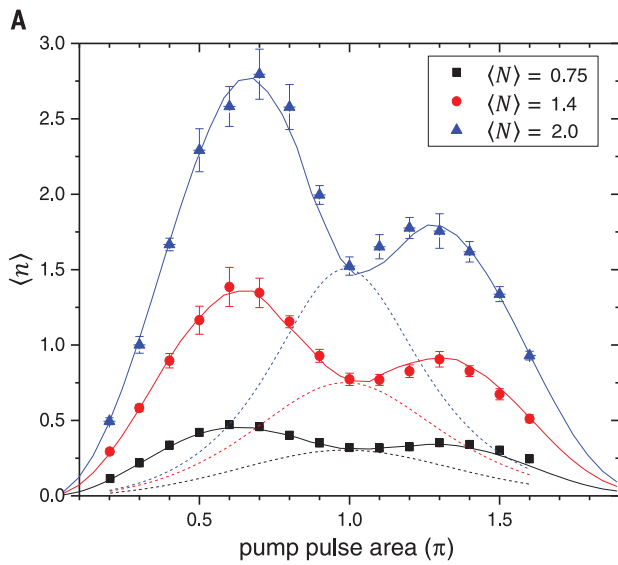


Fig. 2. Intracavity photon number dependence on the atomic state.

(A and B) Intracavity mean photon number $\langle n \rangle$ versus pump pulse area Θ for various mean atom numbers $\langle N \rangle$ in the cavity with (A) phase-aligned atoms and (B) atoms with random phases. The vacuum Rabi angle $g\tau$ is associated with the cavity-enhanced spontaneous emission probability $\sin^2(g\tau)$ during the atom-cavity interaction time τ for a single atom. The

value of $g\tau$ is 0.18 rad for the phase-aligned atoms, averaged over the finite atomic distribution around the antinode of the cavity field, and 0.10 rad for the random-phase atoms with a traveling-wave atom-cavity coupling. Solid (dashed) lines are theoretical predictions for the case of phase-aligned (random-phase) atoms with the actual experimental parameters (17). Error bars indicate SD.

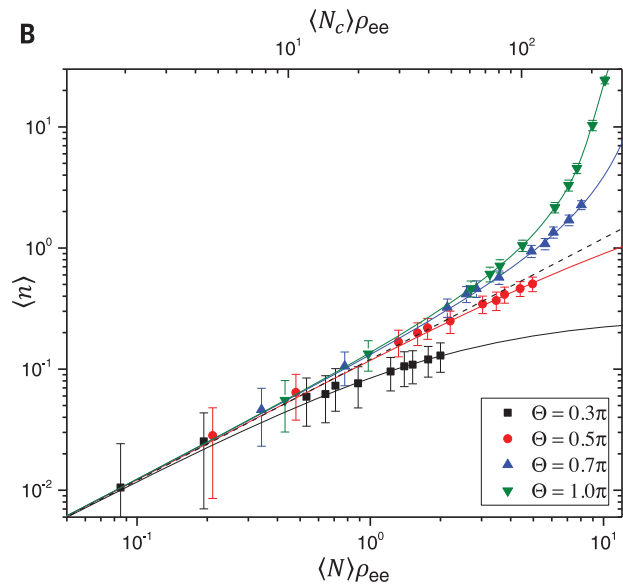
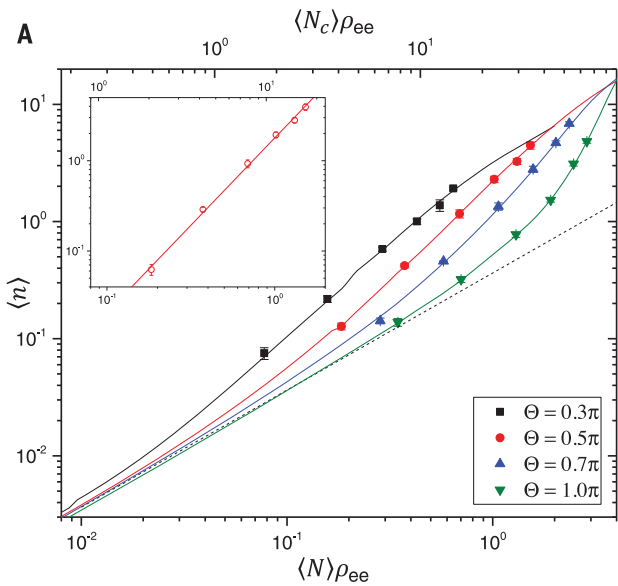


Fig. 3. Intracavity photon number dependence on the number of atoms. (A and B) Intracavity mean photon number $\langle n \rangle$ versus excited-state mean atom number $\langle N \rangle \rho_{ee}$ for (A) the phase-aligned case and (B) the random-phase case. We use $\langle N \rangle \rho_{ee}$ instead of just $\langle N \rangle$ for the horizontal axis to align the noncollective emission contribution as a common baseline. The inset in (A) shows $\langle n \rangle$ with the noncollective contribution subtracted for $\Theta = 0.5\pi$ cases and a linear fit to data with a log-log slope of 1.94 ± 0.04 . Dashed lines correspond to the expected photon number made only by the cavity-enhanced spontaneous emission of atoms. Solid lines denote theoretical predictions with the actual experimental parameters (17). Error bars indicate SD.

corresponding to the dashed line, the recalculated log-log slope becomes 1.94 ± 0.04 (inset of Fig. 3A), which indicates that the observed emission is dominantly superradiance-proportional to the square of the number of atoms. A near-quadratic growth appears even in the negative inversion case of $\Theta = 0.3\pi$, in which only 21% of atoms are in the excited state with the rest in the ground

state. When $\Theta > 0.5\pi$, the atoms have positive population inversion, and thus the photon number grows further by stimulated emission beyond the level reached by the collective emission. In this case, it is impossible to isolate the collective emission effect clearly in the log-log plot.

It is also notable that the log-log slope is almost invariant for a large range of $\langle N_c \rangle$ for

$\Theta \leq 0.5\pi$. The theory predicts that the quadratic dependence on $\langle N_c \rangle$ would be dominant in the region of $(1 + \cos\Theta)^{-1} < \langle N_c \rangle < (g\tau)^{-2}$ for the perfectly phase-aligned atoms, although the practical phase noise would make the domain somewhat reduced. Such a broad-range quadratic growth, occurring independently of $\langle n \rangle$ values, including $\langle n \rangle \ll 1$ as in (23), is a distinctive feature

of the present superradiance compared with the marked slope change occurring near the threshold condition of $\langle n \rangle \approx 1$ in the ordinary lasing case. The absence of the usual lasing threshold or thresholdless lasing in the present superradiance cannot be explained in terms of the so-called β factor in ordinary lasers based on noncollective emission (24). In our experiment, $\beta = (g\tau)^2 \approx 0.034$ in the nanohole-array-aperture case (Figs. 2A and 3A) and 0.011 in the rectangular-aperture case (Figs. 2B and 3B) (17). The latter is consistent with the large mean photon number change occurring at the threshold in Fig. 3B ($\Theta > \pi/2$). Additionally, the range of superradiance or the maximum number of atoms participating in the collective emission can be easily scaled up by choosing smaller $g\tau$ values (fig. S5). This feature may provide a new approach in building thresholdless lasers.

The present single-atom superradiance can be viewed as a consequence of one-sided interaction among a series of atoms separated by tens of meters. The photon emitted by a preceding atom interacts with the next atom after traveling $c\tau/\langle N \rangle$ (about 30 m for $\langle N \rangle = 1$; c , speed of light in a vacuum) when we unfold mirror reflections, although their average distance in real space is only hundreds of micrometers. Due to causality, only the preceding atoms can then affect the quantum states of the following atoms. This interaction induces the emission rate of the atom in the cavity to be twice the emission rate per atom in the usual superradiance (17) (fig. S6).

The time-separated atoms linked by such one-sided interaction can form atom-atom interaction systems, which can serve as a testbed for various quantum many-body physics (25).

The present study deepens our understanding on matter-light collective interaction and provides insight into field-mediated long-range (26, 27) interactions. In addition, the phase-controlled many-atom-field interaction based on the nanohole-array technique can be used in nonclassical field generation such as optical Schrödinger cat states and highly-squeezed vacuum states (28), even in a lossy cavity, contrary to previous studies in the microwave region (29), as well as in realizing superabsorption (30). The greatly enhanced single-atom emission may be useful in constructing efficient quantum interfaces (31).

REFERENCES AND NOTES

1. R. H. Dicke, *Phys. Rev.* **93**, 99–110 (1954).
2. M. Gross, S. Haroche, *Phys. Rep.* **93**, 301–396 (1982).
3. N. Skribanowitz, I. P. Herman, J. C. MacGillivray, M. S. Feld, *Phys. Rev. Lett.* **30**, 309–312 (1973).
4. S. Inouye *et al.*, *Science* **285**, 571–574 (1999).
5. M. Scheibner *et al.*, *Nat. Phys.* **3**, 106–110 (2007).
6. R. Reimann *et al.*, *Phys. Rev. Lett.* **114**, 023601 (2015).
7. M. O. Scully, A. A. Svidzinsky, *Science* **325**, 1510–1511 (2009).
8. R. Röhlberger, K. Schlage, B. Sahoo, S. Couet, R. Ruffer, *Science* **328**, 1248–1251 (2010).
9. S. J. Roof, K. J. Kemp, M. D. Havey, I. M. Sokolov, *Phys. Rev. Lett.* **117**, 073003 (2016).
10. M. A. Norcia, M. N. Winchester, J. R. K. Cline, J. K. Thompson, *Sci. Adv.* **2**, e1601231 (2016).
11. K. Baumann, C. Guerlin, F. Brennecke, T. Esslinger, *Nature* **464**, 1301–1306 (2010).
12. B. Casabone *et al.*, *Phys. Rev. Lett.* **114**, 023602 (2015).
13. A. Neuzner, M. Körber, O. Morin, S. Ritter, G. Rempe, *Nat. Photonics* **10**, 303–306 (2016).
14. J. A. Mlynek, A. A. Abdumalikov, C. Eichler, A. Wallraff, *Nat. Commun.* **5**, 5186 (2014).
15. M. Lee *et al.*, *Nat. Commun.* **5**, 3441 (2014).
16. F. Le Kien, M. O. Scully, H. Walther, *Found. Phys.* **23**, 177–184 (1993).
17. See supplementary materials.
18. W. Choi *et al.*, *Phys. Rev. Lett.* **96**, 093603 (2006).
19. C. Fang-Yen *et al.*, *Phys. Rev. A* **73**, 041802 (2006).
20. K. An, R. R. Dasari, M. S. Feld, *Opt. Lett.* **22**, 1500–1502 (1997).
21. H.-G. Hong *et al.*, *Phys. Rev. Lett.* **109**, 243601 (2012).
22. G. Björk, A. Karlsson, Y. Yamamoto, *Phys. Rev. A* **50**, 1675–1680 (1994).
23. J. G. Bohnet *et al.*, *Nature* **484**, 78–81 (2012).
24. M. Khajavikhan *et al.*, *Nature* **482**, 204–207 (2012).
25. P. Lodahl *et al.*, *Nature* **541**, 473–480 (2017).
26. J. S. Douglas *et al.*, *Nat. Photonics* **9**, 326–331 (2015).
27. Z. Meir, O. Schwartz, E. Shahmoon, D. Oron, R. Ozeri, *Phys. Rev. Lett.* **113**, 193002 (2014).
28. D. Yang, J. Kim, M. Lee, Y.-T. Chough, K. An, *Phys. Rev. A* **94**, 023826 (2016).
29. S. Deléglise *et al.*, *Nature* **455**, 510–514 (2008).
30. K. D. B. Higgins *et al.*, *Nat. Commun.* **5**, 4705 (2014).
31. K. Hammerer, A. S. Sørensen, E. S. Polzik, *Rev. Mod. Phys.* **82**, 1041–1093 (2010).

ACKNOWLEDGMENTS

We thank M. Lee and H.-G. Hong for helpful comments. This work was supported by a grant from the Samsung Science and Technology Foundation under project SSTF-BA1502-05. We declare no competing financial interests. All data needed to evaluate the conclusions in the paper are present in the paper and/or the supplementary materials.

SUPPLEMENTARY MATERIALS

www.sciencemag.org/content/359/6376/662/suppl/DC1
Materials and Methods
Supplementary Text
Figs. S1 to S6
References (32–35)

15 October 2017; accepted 7 December 2017
Published online 21 December 2017
10.1126/science.aar2179

Coherent single-atom superradiance

Junki Kim, Daeho Yang, Seung-hoon Oh and Kyungwon An

Science **359** (6376), 662-666.

DOI: 10.1126/science.aar2179 originally published online December 21, 2017

Building up to superradiance, one by one

Superradiance is a quantum phenomenon that occurs when emitters are sufficiently close to change spontaneous emission. Controlling the position and state of emitters within an atomic ensemble, however, is technically challenging. Kim *et al.* show that spatial correlations can be replaced by temporal correlations to achieve superradiance (see the Perspective by Meschede). They dropped prepared atoms into a high-quality optical cavity and found that the number of photons within the cavity built up superradiantly as the atoms dropped through one by one. The method provides a versatile platform for generating nonclassical states of light.

Science, this issue p. 662; see also p. 641

ARTICLE TOOLS

<http://science.sciencemag.org/content/359/6376/662>

SUPPLEMENTARY MATERIALS

<http://science.sciencemag.org/content/suppl/2017/12/20/science.aar2179.DC1>

RELATED CONTENT

<http://science.sciencemag.org/content/sci/359/6376/641.full>

REFERENCES

This article cites 33 articles, 4 of which you can access for free
<http://science.sciencemag.org/content/359/6376/662#BIBL>

PERMISSIONS

<http://www.sciencemag.org/help/reprints-and-permissions>

Use of this article is subject to the [Terms of Service](#)